M&C 2017 - International Conference on Mathematics & Computational Methods Applied to Nuclear Science & Engineering, Jeju, Korea, April 16-20, 2017, on USB (2017)

Fusion Energy Systems Analysis with the Groupwise Transmutation CADIS Method

Elliott D. Biondo* and Paul P.H. Wilson†

**Oak Ridge National Laboratory, 1 Bethel Valley Rd, Oak Ridge, TN 37830*
†University of Wisconsin — Madison, 1500 Engineering Drive, Madison, WI 53706
biondoed@ornl.gov, paul.wilson@wisc.edu

Abstract - *In fusion energy systems (FES) neutrons born from burning plasma activate system components. The photon dose rate after shutdown from resulting radionuclides must be quantified. This shutdown dose rate (SDR) is calculated by coupling neutron transport, activation analysis, and photon transport. The size, complexity, and attenuating configuration of FES motivates the use of hybrid Monte Carlo (MC)/deterministic neutron transport. The Multi-Step Consistent Adjoint Driven Importance Sampling (MS-CADIS) method can be used to optimize MC neutron transport for coupled multiphysics problems, including SDR analysis, using deterministic estimates of adjoint flux distributions. One implementation of the MS-CADIS method is Groupwise Transmutation (GT)-CADIS which calculates intermediate MS-CADIS parameters through a series of single-energy-group irradiation calculations. This method is expected to perform optimally when important transmutation chains meet a set of criteria referred to as the Single Neutron Interaction and Low Burnup (SNILB) criteria. Previous work involved demonstrating the efficacy of GT-CADIS with a problem consisting of a simple geometry and a single-pulse irradiation scenario. This work demonstrates the application of the GT-CADIS method to a production-level problem. The chosen problem is a Spherical Tokamak Fusion Nuclear Science Facility (ST-FNSF) device operating at 27 MW_{th} with a many-pulse, nine-year irradiation scenario. The SNILB criteria are shown to be met for this scenario and the GT-CADIS method is shown to produce variance reduction parameters tailored for efficiently resolving the neutron flux distribution within important regions of the problem for SDR analysis.*

I. INTRODUCTION

The operation of fusion energy systems (FES) results in neutron activation of system components. Radionuclides produced in this process persist after shutdown and emit decay photons. The potential dose rate from these photons — known as the shutdown dose rate (SDR) — must be quantified as a function of position and time after shutdown for maintenance planning and licensing purposes. The foremost method for calculating the SDR is the mesh-based Rigorous Two-Step (R2S) method [1]. With this method neutron transport is first done in order to obtain a mesh-based multigroup neutron flux distribution over the entire region of interest for activation. Then activation calculations are done for each volume element of the mesh using the irradiation scenario of interest. The activation process results in a mesh-based multigroup photon emission density distribution, which is used as a source for photon transport. By tallying the multigroup photon flux within region(s) of interest, flux-to-dose-rate conversion factors can be used to obtain the SDR.

Both R2S radiation transport steps are challenging due to the physical size, geometric complexity, and attenuating configuration of FES. Deterministic radiation transport methods are ideally suited to resolve particle flux distributions that span many orders of magnitude, as encountered within FES shielding problems. However, these methods require discretization of space, energy, and direction. Computer memory limitations do not permit full-scale deterministic transport for FES applications due the high resolution of discretization required to represent FES geometries and fully capture particle streaming. Monte Carlo (MC) radiation transport allows for continuous treatment of space, energy, and direction, but generally requires the application of MC variance reduction (VR) techniques for transport within the highly-attenuation geometries encountered in FES.

The Consistent Adjoint Driven Importance Sampling (CADIS) method [2] is a hybrid MC/deterministic method that combines the benefits of both transport methods by using a deterministic transport preprocessing step to generate MC VR parameters. With this method, a detector of interest is used as an adjoint source for deterministic adjoint transport. The resulting adjoint flux distribution — which provides an estimate of the importance of phase space regions to the detector response —is used to define MC weight windows and a biased source distribution that optimize MC transport with respect to the detector. The Forward-Weighted (FW)-CADIS method [3] is a method for optimizing MC radiation transport with respect to multiple detectors, or all of space or phase space (i.e., global variance reduction). This is done by using an additional deterministic estimate of the forward flux in order to generate the appropriate adjoint source for use with the standard CADIS method. These methods have been shown to dramatically improve the efficiency of MC simulations for FES applications [4] which motivates the application of these methods to SDR problems.

For the photon transport step of the R2S method the standard CADIS or FW-CADIS method can be applied in order to optimize photon transport for local or global SDR calculations [5]. For R2S neutron transport, global VR techniques have previously been used to evenly distribute MC neutrons throughout all of phase space [5, 6]. FW-CADIS could be used in order to optimize neutron transport using this global approach. However, this global approach is computationally wasteful because not all regions of neutron phase space are of equal importance to the SDR. Instead, neutrons should be directed to regions of phase space that cause neutron activation and subsequently the production of photons at decay times of interest that are important to SDR detector(s). The Multi-Step (MS)-CADIS method [7] can be used to define an adjoint neutron source that, when used with the CADIS method, achieves this optimal neutron biasing. Calculating this adjoint neutron source requires the approximation of the transmutation process.

The Groupwise Transmutation (GT)-CADIS method is an implementation of the MS-CADIS method which uses a series of single-energy-group irradiations to obtain quantities that are used in part to obtain the MS-CADIS adjoint neutron source [8]. This method is effective when the transmutation process meets a set of criteria referred to as the Single Neutron Interaction and Low Burnup (SNILB) criteria. Previous work involved demonstrating the GT-CADIS method for a problem in which the SNILB criteria are met, consisting of a simple geometry and single-pulse irradiation scenario [8]. GT-CADIS provided speedups of 200 ± 100 relative to global variance reduction with the Forward Weighted (FW)-CADIS method and $9 \pm 5 \cdot 10^4$ relative to analog neutron transport.

In this work, the GT-CADIS method is applied to a production-level problem consisting of a realistic FES geometry and irradiation scenario. This demonstration uses the 1 m version of the Princeton Plasma Physics Laboratory (PPPL) Spherical Tokamak Fusion Nuclear Science Facility (ST-FNSF) device [9] with a many-pulse, nine-year irradiation scenario. This small 27 MW (thermal) D-T fusion device has been proposed to further develop fusion blanket technology, namely tritium breeding and thermal power conversion. It is first shown that the SNILB criteria are reasonably met for this problem. GT-CADIS VR parameters are then generated and compared to FW-CADIS parameters. Finally, GT-CADIS VR parameters are used to carry out R2S neutron transport for the calculation of the SDR. For R2S photon transport the standard CADIS method is used to obtain the converged SDR. This work demonstrates that the GT-CADIS method can be applied to production-level problems.

II. METHODOLOGY

The Multi-Step (MS)-CADIS method can be used to optimize neutron transport for coupled multiphysics problems, including SDR analysis.[1] GT-CADIS is one possible implementation of MS-CADIS which uses a series of single-energy-group irradiations to approximate the transmutation process. With this method, it is assumed that the decay photon emission density in photon energy group h within discrete volume v can be approximated by the following relationship:

$$q_{v,p,h} = \sum_g T_{v,g,h}\, \phi_{v,n,g}, \tag{1}$$

where $\phi_{v,n,g}$ is the neutron flux in neutron energy group g within volume v and $T_{v,g,h}$ is a constant that depends only on the material within v and the irradiation scenario. This relationship cannot accurately describe a generic transmutation process because for arbitrary transmutation networks the relationship between neutron flux and decay photon emission density is nonlinear. If values for $T_{v,g,h}$ can be found such that Equation 1 provides a reasonable approximation for the decay photon emission density, the following adjoint neutron source ($q^+_{v,n,g}$) — adapted from Ibrahim et al. [7] — can be used with the CADIS method to accelerate neutron transport:

$$q^+_{v,n,g} = \sum_h T_{v,g,h}\, \phi^+_{v,p,h}. \tag{2}$$

Here, $\phi^+_{v,p,h}$ is the adjoint photon flux which can be estimated deterministically using the SDR detector as an adjoint photon source.

GT-CADIS provides a procedure for calculating $T_{v,g,h}$ values for use with Equation 2. For each material in the problem irradiations are carried out using the irradiation scenario of interest with neutron fluxes containing neutrons only in energy group g. The resulting decay photon emission density in energy group h is denoted by $q_{p,h}(\phi_{n,g})$ and is used to calculate the material-specific quantity $T_{g,h}$:

$$T_{g,h} = \frac{q_{p,h}(\phi_{n,g})}{\phi_{n,g}}. \tag{3}$$

This process is done for all g and h. The $T_{v,g,h}$ can then be calculated by mapping $T_{g,h}$ into the spatial domain:

$$T_{v,g,h} = T_{g,h} \text{ for material in } v. \tag{4}$$

This process for calculating $T_{v,g,h}$ is only valid when the transmutation chains that result in the production of important photons have the following properties:

1. The first, and only the first, transmutation process in the chain is the result of a neutron interaction,
2. The irradiation time is sufficiently short such that significant depletion of any nuclides in the chain does not occur.

These criteria are referred to as the Single Neutron Interaction and Low Burnup criteria (SNILB). The mathematical basis for these criteria and their relationship to the GT-CADIS method are detailed elsewhere [8]. Since $T_{v,g,h}$ are used for the purpose of MC VR, minor violations in the SNILB criteria may be acceptable because VR parameters only affect the efficiency of MC transport and not the converged result (provided that they are not so poor that they cause significant undersampling). To this end, a heuristic method for quantifying the extent to which the SNILB criteria are met has been proposed [8]. For a given material, a series of single-energy-group irradiations are carried out with the irradiation scenario of interest for each energy group in a characteristic neutron spectrum. The photon emission density for each photon group, h, $q_{p,h}(\phi_{n,g})$, is recorded. A final irradiation is conducted using all neutron energy groups in the neutron spectrum simultaneously in order to obtain $q_{p,h}(\phi_n)$. By estimating the importance of each photon energy group, I_h, the quantity η_I is defined:

[1] From this point forward, all references to the MS-CADIS method imply the application of the MS-CADIS method to SDR analysis, specifically.

$$\eta_I = \frac{\sum_g \sum_h q_{p,h}(\phi_{n,g}) I_h}{\sum_h q_{p,h}(\phi_n) I_h}. \tag{5}$$

This quantity will equal one if the SNILB criteria are met. If η_I is less than or greater than one, the GT-CADIS method will either underestimate or overestimate the importance of the material to the detector response, respectively. The I_h used in this formulation are equivalent to the energy spectrum of the adjoint photon flux with respect to a photon detector, which is application-specific and may vary widely throughout a particular problem. Forgoing the inclusion of transport affects, flux-to-dose-rate conversion factors provide a convenient function to use for I_h. For the purpose of this work, a set of ICRP-74 [10] flux-to-dose-rate conversion factors recommended by the ITER organization [11] were used for I_h.

In this work the GT-CADIS method is carried out with a collection of physics codes. All MC transport was done with the Direct Accelerated Geometry Monte Carlo (DAGMC) version of MCNP5 [12] (DAG-MCNP5) which facilitates MC radiation transport directly on CAD geometry [13]. A custom source sampling subroutine was compiled into DAG-MCNP5 in order to allow for the use of mesh-based sources, with analog and biased random sampling [5]. FENDL-2.1 nuclear data was used for all MC transport. All deterministic transport was carried out with the PARTISN 4.00 3D S_N code [14], using P_5S_{16}, FENDL-2.1 nuclear data, and the VITAMIN-J group structure (175 neutron groups, 42 photon groups) [15]. Activation was done with ALARA [16] with FENDL/A-3.0 [17] nuclear data. Automatic coupling of these physics codes was facilitated by code contributed to the Python for Nuclear Engineering (PyNE) toolkit [18], including the PyNE R2S workflow [5], and PARTISN input generation capabilities [19].

III. PROBLEM DESCRIPTION

To demonstrate the GT-CADIS method an SDR problem was created using the 1 m version of the PPPL ST-FNSF [9]. A CAD model of this geometry is shown Fig. 1 and annotated with material assignments, some of which are homogenized mixtures. This model features homogenized breeding zones, blanket modules, center stack, and other components. Though the proposed device is not exactly symmetric vertically or toroidally, an octant of the geometry with reflective boundaries was chosen for this demonstration, allowing for a finer mesh resolution to be used. Fig. 1 also shows the chosen location of the photon dose rate detector. This detector is sufficiently far from the reflecting boundaries that asymmetric effects are not expected to be significant.

The neutron source is a burning D-T plasma confined within the device. A mesh-based neutron source was generated in order to employ biased neutron source sampling via the PyNE source sampling capabilities. For this purpose (and the rest of this problem) a nonuniform 62×62×69 Cartesian mesh (265,236 mesh volume elements) was created by hand to conform to important geometry boundaries. A mesh-based neutron source was obtained using plasma source capabilities within DAGMC [20]. These capabilities allow for the random sampling of the initial positions and energies of neutrons born from plasma. Using a low-confinement (L) mode model, 10^8 particles were sampled. These particles were tallied onto the mesh in the VITAMIN-J 175 energy group format. Using this tallied information as well as the volume of each mesh volume element, a probability density function (PDF) of the neutron source density was created. The PDF for the dominant energy group (13.8–14.2 MeV) is shown in Fig. 2. This figure (and the remaining figures in this section) show a slice through the geometry at a 45° angle.

The total source intensity of the octant was chosen to be $1.197 \cdot 10^{18}$ n/s, which corresponds to 27 MW of fusion power within the full device. A complex irradiation scenario was chosen, as shown in Fig. 3. This scenario consists of approximately nine years of pulsed irradiation, followed by a one-day cooldown period, which are relevant time scales for FES operation and maintenance planning.

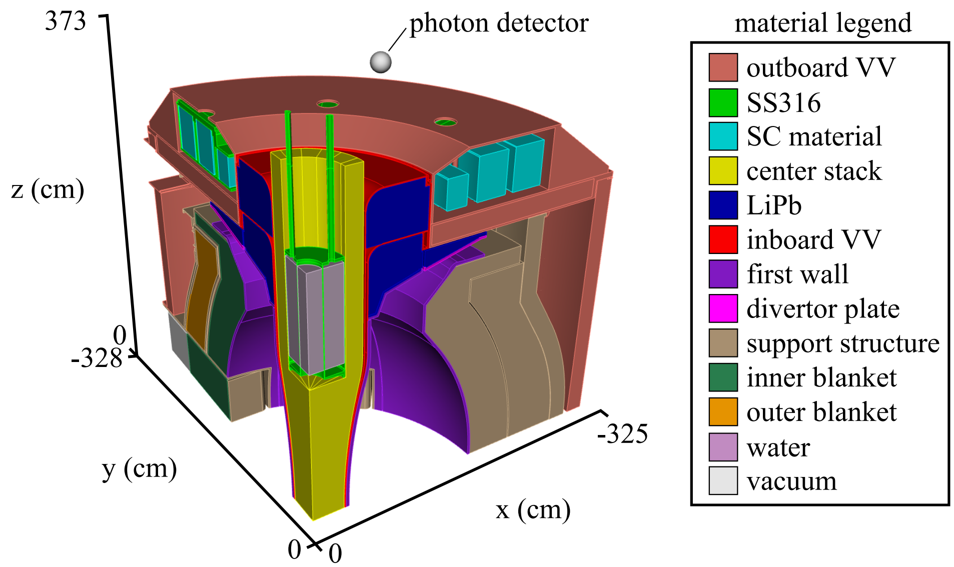

Fig. 1: Octant of the 1 m ST-FNSF labeled with material assignments. Here “VV” denotes vacuum vessel and “SC” denotes superconducting.

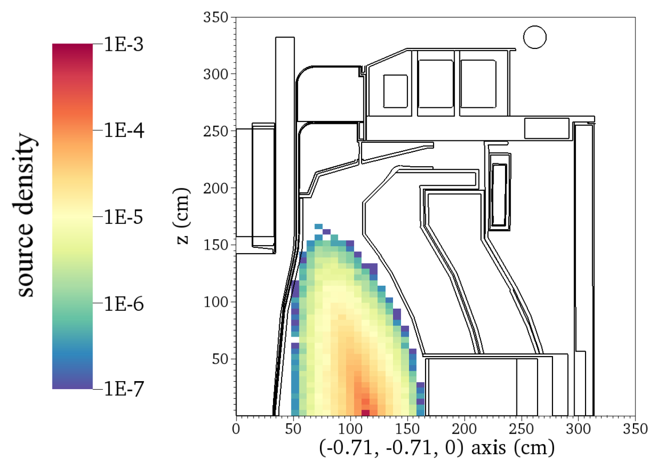

Fig. 2: Neutron source density PDF for the 13.8 – 14.2 MeV energy group.

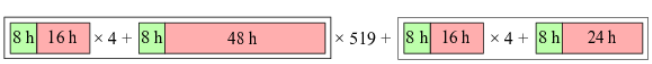

Fig. 3: Scenario consisting of approximately nine years of pulsed irradiation, followed by a 1 day shutdown period. Green represents irradiation intervals and red represents decay intervals.

IV. RESULTS AND DISCUSSION

Prior to generating GT-CADIS neutron VR parameters, the SNILB criteria were evaluated in order to assess the expected efficacy of the GT-CADIS method. This was done by evaluating η_I for each material using the irradiation scenario from Fig. 3 and characteristic first wall, shield, and vacuum vessel neutron spectra [8]. Resulting η_I values are shown in Table I. This table shows that for all spectra and materials, all η_I are within 4% of 1.0. This indicates that the SNILB criteria are reasonably met in this case and that the GT-CADIS method will perform optimally.

To generate GT-CADIS VR parameters a deterministic

TABLE I: Values of η_I for the 1 m ST-FNSF materials for characteristic neutron spectra and the irradiation scenario from Fig. 3. ICRP-74 flux-to-dose-rate conversion factors were used for I_h.

	η_I		
Material	first wall	shield	vacuum vessel
outboard VV	1.02	1.00	1.00
SS316	1.04	1.00	1.00
SC material	1.03	1.01	1.00
center stack	1.00	1.00	1.00
LiPb	1.02	1.00	1.00
inboard VV	1.02	1.00	1.00
first wall	1.02	0.99	1.00
divertor plate	0.97	1.00	1.00
support structure	1.02	1.00	1.00
outer blanket	1.02	1.00	1.00
inner blanket	1.02	1.00	1.00
water	1.00	1.00	1.00

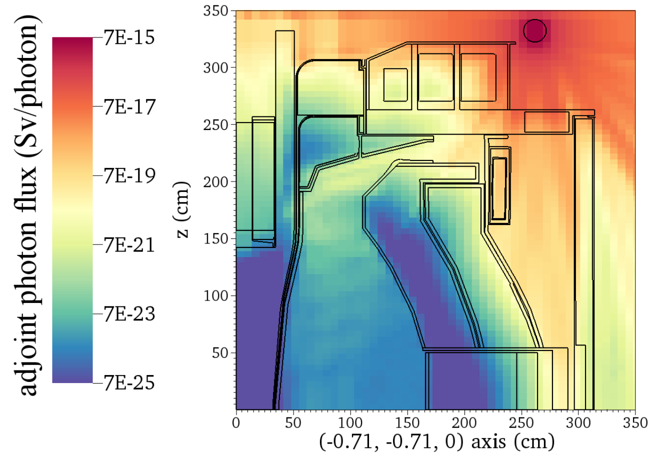

Fig. 4: Adjoint photon flux distribution for the 0.8 – 1.0 MeV energy group.

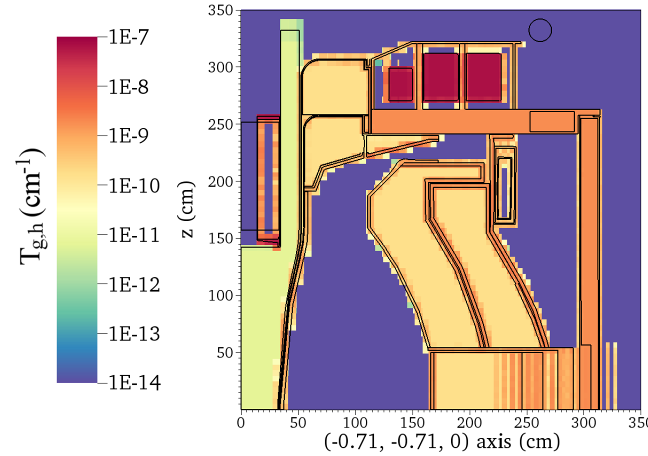

Fig. 5: $T_{g,h}$ distribution for the 1.0–1.11 MeV neutron energy group (g) and the 0.8 – 1.0 MeV photon energy group (h).

adjoint photon transport calculation was first done using the detector shown in Fig. 1 as the adjoint source with ICRP-74 flux-to-dose-rate conversion factors defining the adjoint source spectrum. This required the discretization of the CAD geometry in Fig. 1 onto the Cartesian mesh for use with PARTISN. Since the Cartesian mesh does not conform to the geometry, many mesh volume elements contain multiple geometry cells — and in many cases multiple materials — resulting in a large number of unique material mixtures. Due to computer memory limitations, this collection of mixtures was collapsed down into a smaller set of approximate mixtures. This was done using a 25% relative tolerance.[2] PARTISN was run with 4 computer cluster nodes with 16 MPI processes per node. Each node was an Intel® Xeon® E5-2670 v2 CPU with a clock speed of 2.50 GHz and 128 GB of RAM. The adjoint photon flux distribution is shown in Fig. 4.

Next, T was calculated for all of the materials in the problem for the irradiation scenario of interest. These T were then mixed by volume fraction in order to obtain a T for each mesh volume element. This was done using the actual volume fractions within each mesh volume element — not the approximate volume fractions used for generating PARTISN input. Fig. 5 shows the $T_{g,h}$ distribution for the 1.0–1.11 MeV neutron energy group (g) and the 0.8 – 1.0 MeV photon energy group (h). This figure shows that $T_{g,h}$ for the superconducting material (poloidal field coil) is approximately two orders of magnitude greater than any other material for this particular g and h. (The striped patterns in the bottom of the plot are a result of the 45° slice through the geometry, which intersects mesh volume elements diagonally.)

The T for each mesh volume element and the adjoint photon flux distribution were used to calculate the GT-CADIS adjoint neutron source distribution, shown in Fig. 6a, via Equation 2. This figure shows that the most important spatial regions for neutrons are the areas of the PF coil and structural material in the immediate vicinity of the detector. For the purpose of comparison, an adjoint neutron source was also calculated via the FW-CADIS method (in this case for global variance reduction across phase space), shown in Fig. 6b. As expected, the adjoint source intensity is inversely proportional to the forward flux. Since the detector happens to be in the region of lowest forward flux in this problem, the FW-CADIS method would likely provide a speedup over analog. However, unlike GT-CADIS, the FW-CADIS adjoint neutron source has high intensity in regions of low importance (e.g., the inboard and the region behind the vacuum vessel) which will result in MC neutrons wastefully being directed toward these regions.

Deterministic adjoint neutron transport was then carried out with the same run configuration and mixture collapsing criterion as adjoint photon transport. Using the resulting adjoint neutron flux distribution, neutron weight windows and a biased source were generated, as shown in Fig. 7a and 7b. The weight window distribution suggests that streaming through the gap below the divertor plate is a more important pathway than diffusion through first wall and outboard blanket modules. It also shows that the neutron importance is nearly uniform throughout the plasma region. Likewise, the biased neutron source distribution is nearly identical to the unbiased source distribution shown in Fig. 2, indicating that neutron source biasing is not particularly important for this problem.

In to order calculate the SDR, MC neutron transport was first done using the GT-CADIS weight windows and biased source. This was done using the same hardware as deterministic transport but with 8 nodes and 20 MPI tasks per node. A total of $2{\cdot}10^9$ particles were simulated in 311 days of CPU time.[3] The total neutron flux distribution is shown in Fig. 8a. This figure shows that the total neutron flux is attenuated by approximately 5 orders of magnitude between the

[2] In other words, if the volume fractions of the all the materials within two mixtures were within 25% of each other, these two mixtures were represented by a single mixture.

[3] During neutron transport an average of 1 in 5,600 particles were lost. Further analysis indicated that these lost particles were not confined to any single region, indicating significant issues with the CAD geometry. For FES analysis lost particles are common, and the loss rate must be weighed against the significance of the calculation. Since neutron flux and relative error distributions are consistent with expectations, this loss rate was deemed acceptable for the purpose of this demonstration.

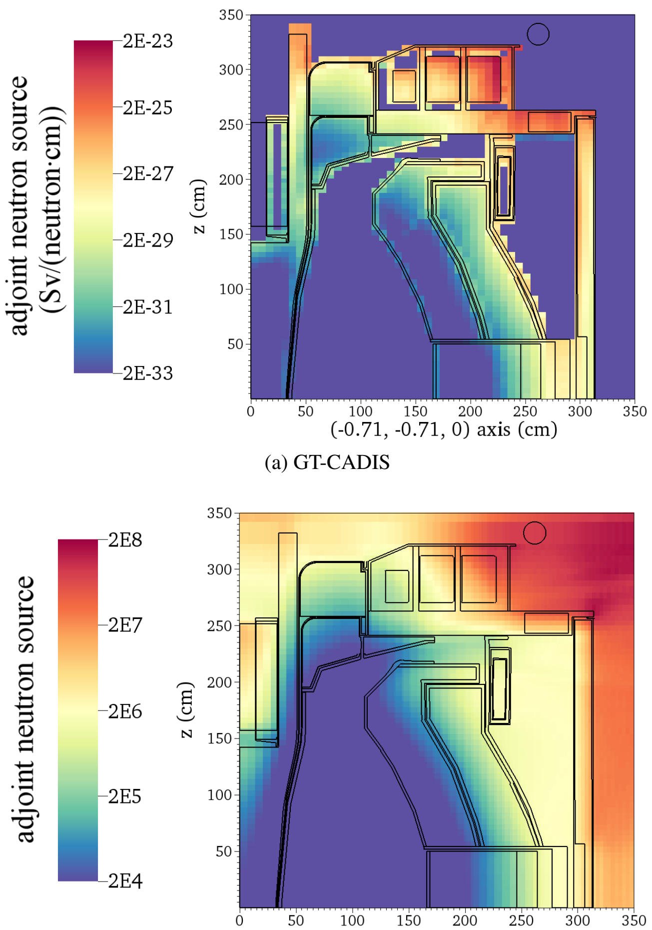

(a) GT-CADIS

(b) FW-CADIS

Fig. 6: Adjoint neutron source distributions for the 1.0 – 1.11 MeV energy group.

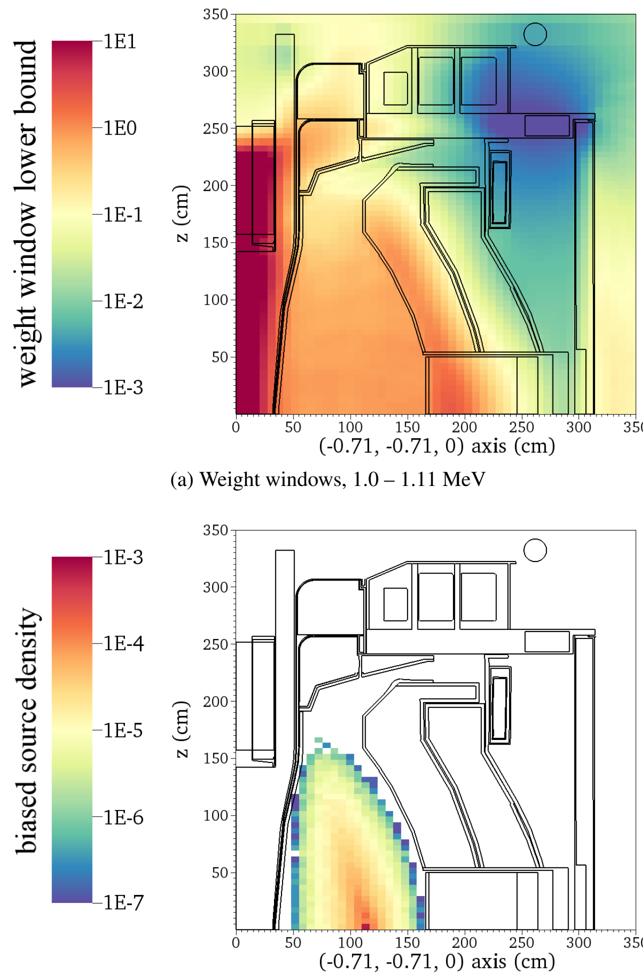

(a) Weight windows, 1.0 – 1.11 MeV

(b) Biased source, 13.8 – 14.2 MeV

Fig. 7: GT-CADIS neutron VR parameters.

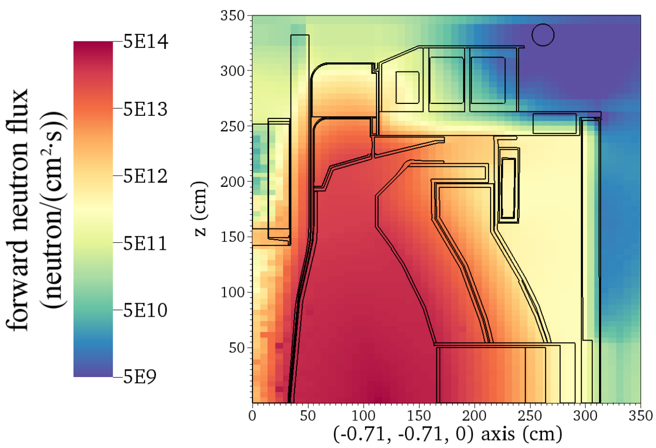

(a) Total neutron flux

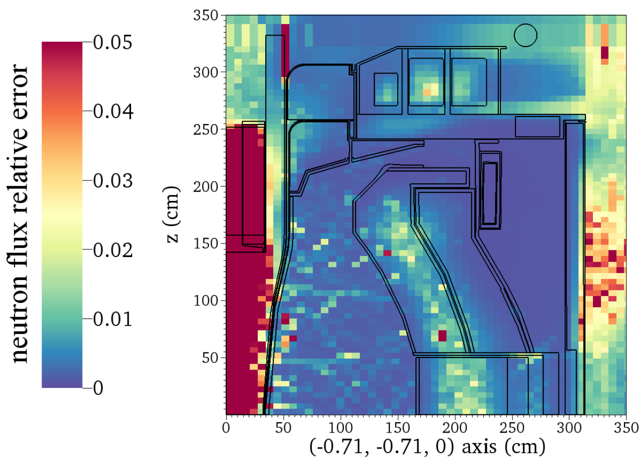

(b) Total neutron flux relative error

Fig. 8: Forward neutron transport results.

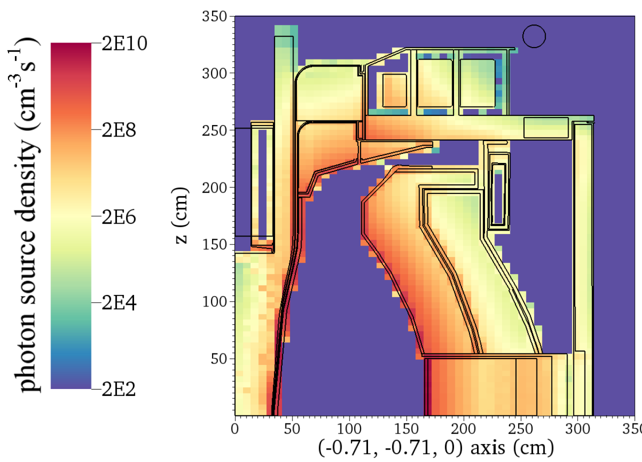

(a) Unbiased

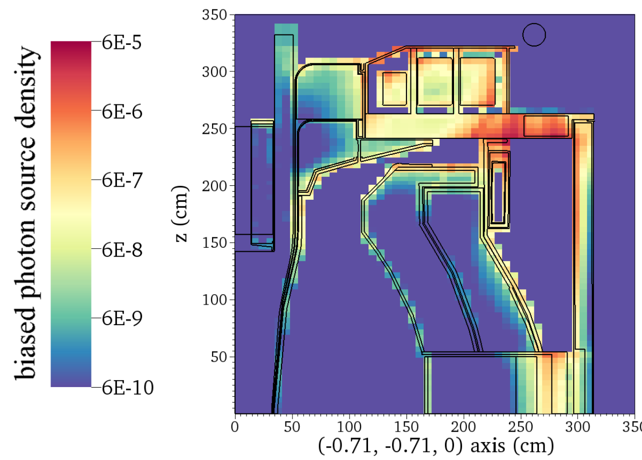

(b) Biased with CADIS

Fig. 9: Photon emission density distributions for the 0.8 – 1.0 MeV energy group.

source and detector. The corresponding relative error distribution in Fig. 8b shows that significantly less processor time is spent simulating particles in low-importance regions such as the center stack, outboard breeding zones, and deep within the PF coils. A region of lower relative error is seen outwards of the outer PF coil. This is due to the fact that the PF coils block streaming high-weight particles that increase the variance in the surrounding vacuum regions. Relative errors are less than 1% in the most important regions (i.e., regions where the weight windows are low in Fig. 7a).

Using PyNE R2S, ALARA input was generated and ALARA was run for each mesh volume element. The resulting photon emission density is shown in Fig. 9a. This figure shows that the first wall has 2–3 orders of magnitude greater photon emission density than the important regions of the problem (i.e., regions of high adjoint photon flux in Fig. 4). For this reason, the standard CADIS method was used to generate weight windows and a biased source for photon transport. The biased photon source, shown in Fig. 9b, results in preferential sampling of MC photons in the region near the photon dose rate detector. Since the adjoint photon flux distribution was already required for GT-CADIS, no additional deterministic transport was required for this step.

Photon transport was done using the standard CADIS weight windows and biased source with 10^{10} particles simulated on the same hardware configuration as neutron transport.[4] Photon transport required 48.0 days of CPU time and resulted in a converged SDR of $4.02 \cdot 10^{-5}$ Sv/s with a photon transport relative error of 0.0014. The calculated SDR for this problem is extremely high: these results indicate that after approximately nine years of operation at full power, a much longer cooldown time should occur in order to perform any maintenance operations.

V. CONCLUSION

This work details the process of how the GT-CADIS method can be used in practice. A realistic geometry and irradiation scenario were chosen. The quantity η_I was first evaluated for each material in the problem using the irradiation scenario of interest and characteristic FES neutron spectra. This process provided *a priori* knowledge that the SNILB criteria

[4]Photon transport resulted in fewer lost particles than neutron transport: only 1 in $2.01 \cdot 10^5$.

are reasonably met for this problem and that the GT-CADIS method would be effective. Weight windows and a biased source were then generated using GT-CADIS. The resulting weight window distribution took on the expected shape — clearly biasing neutrons toward the important regions of the problem. The similarity between the biased source and unbiased sources indicates that source biasing may not be paramount for this class of problem. The use of the GT-CADIS method also allowed for the standard CADIS method to be employed for photon transport without any additional deterministic transport steps. It is clear that the GT-CADIS method can and should be applied to production-level problems, much like the standard CADIS and FW-CADIS methods, which are in wide use today.

VI. ACKNOWLEDGMENTS

This work was funded in part by project DE-FG02-99ER54513 from the U.S. DOE Office of Fusion Energy Sciences and by the U.S. Nuclear Regulatory Commission Fellowship program. This research was performed using the compute resources and assistance of the UW-Madison Center For High Throughput Computing (CHTC) in the Department of Computer Sciences. The CHTC is supported by UW-Madison and the Wisconsin Alumni Research Foundation, and is an active member of the Open Science Grid, which is supported by the National Science Foundation and the U.S. Department of Energy's Office of Science.

REFERENCES

1. A. DAVIS and R. PAMPIN, "Benchmarking the MCR2S system for high-resolution activation dose analysis in ITER," *Fusion Engineering and Design*, **85**, *1*, 87–92 (2010).
2. A. HAGHIGHAT and J. C. WAGNER, "Monte Carlo Variance Reduction with Deterministic Importance Functions," *Progress in Nuclear Energy*, **42**, *1*, 25–53 (2003).
3. J. C. WAGNER, D. E. PEPLOW, and S. W. MOSHER, "FW-CADIS Method for Global and Regional Variance Reduction of Monte Carlo Radiation Transport Calculations," *Nuclear Science and Engineering*, **176**, *1*, 37–57 (2014).
4. A. M. IBRAHIM, P. P. WILSON, M. E. SAWAN, S. W. MOSHER, D. E. PEPLOW, and R. E. GROVE, "Assessment of fusion facility dose rate map using mesh adaptivity enhancements of hybrid Monte Carlo/deterministic techniques," *Fusion Engineering and Design*, **89**, *9–10*, 1875–1879 (2014), Proceedings of the 11th International Symposium on Fusion Nuclear Technology-11 (ISFNT-11) Barcelona, Spain, 15–20 September, 2013.
5. E. D. BIONDO, A. DAVIS, and P. P. H. WILSON, "Shutdown dose rate analysis with CAD geometry, Cartesian/tetrahedral mesh, and advanced variance reduction," *Fusion Engineering and Design*, **106**, 77–84 (2016).
6. A. TURNER, R. PAMPIN, M. LOUGHLIN, Z. GHANI, G. HURST, A. L. BUE, S. MANGHAM, A. PUIU, and S. ZHENG, "Nuclear analysis and shielding optimisation in support of the ITER In-Vessel Viewing System design," *Fusion Engineering and Design*, **89**, *9–10*, 1949–1953 (2014).
7. A. M. IBRAHIM, D. E. PEPLOW, R. E. GROVE, J. L. PETERSON, and S. R. JOHNSON, "The Multi-Step CADIS Method for Shutdown Dose Rate Calculations and Uncertainty Propagation," *Nuclear Technology*, **192**, *3*, 286–298 (2015).
8. E. D. BIONDO and P. P. H. WILSON, "Transmutation Approximations for the Application of Hybrid Monte Carlo/Deterministic Neutron Transport to Shutdown Dose Rate Analysis," *Nuclear Science and Engineering* (In press 2017).
9. T. BROWN, J. MENARD, L. E. GUEBLAY, and A. DAVIS, "PPPL ST-FNSF Engineering Design Details," *Fusion Science and Technology*, **68** (Sept. 2015).
10. "Conversion Coefficients for use in Radiological Protection against External Radiation," *ICRP Publication 74*, **26**, *3/4* (1996).
11. M. J. LOUGHLIN, "Recommendations on Computation of Dose from Flux Estimates," Tech. Rep. IDM Number ITER_D_29PJCT, ITER (2008).
12. X-5 MONTE CARLO TEAM, "MCNP - A General Monte Carlo N-Particle Transport Code, Version 5," (2004).
13. T. J. TAUTGES, P. P. H. WILSON, J. KRAFTCHECK, B. F. SMITH, and D. L. HENDERSON, "Acceleration Techniques for Direct Use of CAD-Based Geometries in Monte Carlo Radiation Transport," in "International Conference on Mathematics, Computational Methods & Reactor Physics (M&C 2009)," American Nuclear Society, Saratoga Springs, NY (2009).
14. R. ALCOUFFE, R. BAKER, J. DAHL, S. TURNER, and R. WARD, "PARTISN: A Time-Dependent, Parallel Neutral Particle Transport Code System," Tech. Rep. LA-UR-05-3925 (May 2005).
15. E. SARTORI and G. PANINI, "ZZ GROUPSTRUCTURES, VITAMIN-J, XMAS, ECCO-33, ECCO2000 Standard Group Structures," Tech. Rep. 40-03, Nuclear Energy Agency of the OECD (NEA) (1991).
16. P. P. H. WILSON, H. TSIGE-TAMIRAT, H. Y. KHATER, and D. L. HENDERSON, "Validation of the ALARA activation code," *Fusion Technology*, **34**, *3*, 784–788 (1998).
17. J. KOPECKY, "VALIDATION OF FENDL-3/A LIBRARY USING INTEGRAL MEASUREMENTS," Tech. Rep. INDC(NED)-011, IAEA INDC International Nuclear Data Committee, Vienna, Austria (2012).
18. C. BATES, E. BIONDO, K. HUFF, K. KIESLING, and A. SCOPATZ, "PyNE Progress Report," *Transactions of the American Nuclear Society*, **111** (2014).
19. K. R. KIESLING, A. DAVIS, and P. P. H. WILSON, "PyNE: Usage for Automatic PARTISN Input File Generation from a CAD Geometry," *Transactions of the American Nuclear Society*, **113**, 1029–1032.
20. A. DAVIS, "DAGMC plasma sources," `https://github.com/makeclean/DAGMC/tree/plasma_sources/sources` (2016).